Accepted by the Journal of Vacuum Science and Technology B.
Assigned JVST Manuscript #11599.

Atomic Fluorine Beam Etching Of Silicon And Related Materials

P.R. Larson, K.A. Copeland, G. Dharmasena, R.A. Lasell, M. Keil,
and M.B. Johnson
Department of Physics and Astronomy
University of Oklahoma
Norman, Oklahoma 73019

A 1 eV neutral atomic fluorine beam has been shown to produce etch rates in silicon as high as 1 μm/min. Using a CaF_2 resist layer we fabricated 120 μm-deep by 1 μm-wide trenches (aspect ratio 120:1) in silicon with little sidewall taper (slopes of about 1000:1) or aspect-ratio dependent etching effects. Achieving such anisotropic etching suggests that the scattered species do not contribute significantly to sidewall etching under the conditions of this experiment. We estimate that the ultimate depth attainable for a 1 μm-wide trench is about 250 μm and that the critical parameter for attaining a trench of a certain depth is the aspect ratio. Our observations and analysis suggest that this etching technique can be used to fabricate trenches on a nanoscale level while maintaining high aspect ratios of 100 or greater.

I. INTRODUCTION

The ability to etch highly anisotropic features in silicon has been, and will continue to be, a crucial requirement for the size reduction of devices in integrated circuits. Currently, dry etching techniques such as plasma etching and reactive ion etching are used to transfer patterns into device substrates. These techniques have had remarkable success in fabricating highly anisotropic features, but they suffer from several disadvantages affecting their ability to etch such structures on a still smaller scale. These disadvantages include: substrate damage due to charging and ion bombardment, feature-size dependence on the etch rate, and undercutting due to sidewall charging and scattering of reactive species.[1,2] Recently, atomic beam techniques have been developed[3-7] that have the ability to etch anisotropic features into substrates.[5] With their relatively simple chemistry and use of low energy neutral atoms, these techniques do not suffer from several of the disadvantages listed above.

In this report, we describe an application of an intense atomic fluorine beam to rapidly etch silicon and related materials. In addition, we conduct experiments that utilize the inherently collimated nature of atomic beams to fabricate extremely anisotropic etching features.

II. EXPERIMENTAL DETAILS

Figure 1 shows the atomic fluorine beam etching apparatus, which has been described elsewhere in detail.[3] The apparatus consists of an atomic fluorine source connected via differential pumping to a target chamber. Diffusion pumps using fully fluorinated Fomblin oils evacuate both vacuum chambers. The target chamber pump is *l*N_2 baffled, and the pressure in this chamber is about $2x10^{-5}$ Torr ($5x10^{-6}$ Torr) while the beam is on (off). To generate a well-collimated, intense beam, we thermally dissociate a high-pressure (2000-3000 Torr) gas mixture of 5% F_2 in He

flowing through a ~150 μm-diameter nozzle at the tip of a MgF_2 tube. Heating the nozzle to ~900°C results in a measured dissociation yield of about 70%.[3] The kinetic energy of the atomic F beam is measured to be 1.0±0.1 eV. Downstream, the jet is collimated by a 750 μm-diameter skimmer before reaching the sample target. Beam intensities are difficult to measure directly;[8] based on flow measurements for the He beam component we estimate (within a factor of 2) an F intensity of $1x10^{18}$ $cm^{-2}s^{-1}$. Samples are cleaned using a standard degreasing treatment (acetone, methanol, and DI water); in the case of Si samples this is followed by a dilute HF etch to remove any surface oxides. The samples are then mounted onto a resistively heated copper target assembly and loaded into the etching chamber.

It is useful to comment on the effects that our very-high, rather than ultra-high, vacuum conditions may have on our etching process. In general, vacuum conditions affect an etching process either: 1) through the continual contamination of the etching surface, while etching is taking place; or 2) through the initial build-up of a contamination layer before the etching process has been started. The effect our non-UHV conditions have through mechanism 1) may be estimated by comparing the atomic fluorine beam flux on the sample to the flux of other vacuum constituents. Residual gas analysis of the $5x10^{-6}$ Torr background vacuum indicates it is nearly entirely composed of water and air. Using the usual monolayer formation rate of one per second at $1x10^{-6}$ Torr, we find that the flux associated with water and air is $1x10^{16}$ $cm^{-2}s^{-1}$, or the flux ratio of atomic fluorine to water and air is 100:1. Regarding oil backstreaming from the cold-trapped diffusion pump, the Fomblin oil partial pressure is about 10^{-8} Torr, as given by the vapor pressure of Fomblin oil at our chamber temperature of about 25°C.[9] Thus the flux ratio of atomic fluorine to Fomblin oil is $5x10^{4}$:1. Such large flux ratios are due to the highly directional nature of the intense atomic fluorine beam. These flux ratios imply that *once etching begins* the effect of water and air

in direct etching will be small and the effect of Fomblin vapor will be negligible. On the other hand, through mechanism 2), a thin layer of Fomblin oil initially present on the sample at room temperature may protect the substrate and partially inhibit etching until the oil is removed by heating the sample to some threshold temperature, that depends on the vacuum conditions. Such behavior is supported by the fact that the vapor pressure of Fomblin oil at 100^{o}C is about four orders of magnitude larger than at room temperature, so that at elevated sample temperatures one expects the layer of Fomblin oil to reduce in thickness or disappear entirely. In fact, we have directly observed evidence of the presence of a contamination layer in two ways. Firstly, as we have improved our vacuum conditions (*e.g.,* by using a cold-trap on the diffusion pump and using sorption pumps to rough the etching chamber, rather than a mechanical pump) we have observed a reduction of this threshold temperature from about 150^{o}C to below 80^{o}C. Secondly, by initiating etching with a sample temperature at 120^{o}C and quickly reducing this temperature to 25^{o}C, while continuing to etch the sample, we *directly* observe room temperature etching at the expected rate. (This result is discussed in more detail in the Results Section.) In summary, the only effect of our very-high vacuum conditions that we observe is a thin contamination layer that initially inhibits etching. To eliminate the effect of this layer, unless otherwise stated, all of the results reported here are for substrate temperatures at or above 120^{o}C, where the observed effect is negligible; and for our best possible very-high vacuum conditions.

III. RESULTS

Figure 2(a) shows etch depths versus time for silicon and related materials at a substrate temperature (T_{SUB}) of 120^{o}C. Etch depths were measured by etching through a nickel grid, with 0.5 mm openings and 0.75 mm period, using a Tencor Profilometer to measure step heights. Etch rates

were determined by etching samples for various time intervals. The spread in the data is due to run-to-run variations in the atomic flux arising from changes in the beam-source nozzle temperature and pressure. (Thermal dissociation of F_2 is highly sensitive to both temperature and pressure.) Typical run-to-run etch-rate variations for the same nominal conditions are about 20%, while variations within the same run are lower.

Measured etch rates for silicon, silicon nitride, and silicon dioxide for a substrate temperature of 120^{o}C are 0.2, 0.08, and 0.03 μm/min, respectively.[10] Typical photoresist materials etch at the rates shown in the table inset in Fig. 2(a), which also shows their etch selectivities compared to silicon. Fully fluorinated materials such as Teflon and CaF_2, and materials such as Ni that form non-volatile fluorides, do not etch even at temperatures well above 100^{o}C.

Figure 2(b) shows a plot of etch rate versus sample temperature, for temperatures from 80 to 500^{o}C (solid squares), plotted in the usual Arrhenius form. The good straight-line fit (solid line) through our data indicates a substrate-temperature-activated process with activation energy of 0.1 eV as given by the slope. An etch rate as high as 1 μm/min for silicon is observed for T_{SUB}=500^{o}C. For a substrate temperature of 25^{o}C and etch time of 15 minutes, the etching rate directly measured was $9x10^{-4}$ μm/min, two orders of magnitude lower than the etch rate expected for Arrhenius behavior. This is most likely explained by a thin protective layer of Fomblin oil that inhibits the etching. To demonstrate the existence of a contamination layer and that this layer can be removed effectively by heating the sample to 120^{o}C, we first etched for 5 minutes at 120^{o}C, then cooled the sample to 25^{o}C in about 2.5 minutes with the fluorine beam still on, and finally, continued etching for one hour. For this procedure, the cumulative depth etched was observed to be 4.6 μm, much deeper than expected if only the etching at 120^{o}C was effective. The depth attributable to room temperature etching was determined by subtracting the known depth for

etching at 120°C for 5 min. (1.1 μm, as measured in this run), and the depth for etching during the 2.5 min. cool down (0.3 μm, using etch rates at three intermediate temperatures determined by extrapolation). This gives us a room temperature etch rate of 0.06 μm/min which agrees well with the Arrhenius behavior, as shown in Fig. 2(b). The difference between the two room-temperature measurements directly indicates the presence of a thin layer of contamination that inhibits etching during direct room temperature etching, which however, is removed by first initiating etching at 120°C. Finally, for comparison, on the Arrhenius plot in Fig. 2, we also shows results from Flamm *et al.*[11] (dotted line) for atomic fluorine gas etching, and Giapis *et al.*[5] (solid circle) for atomic fluorine beam etching. All these results have been normalized to our flux to compare etching efficiencies. Detailed comparisons of these different etching techniques are left to the Discussion Section below.

The roughness of etched surfaces was measured by atomic force microscopy. A Si(100) sample etched for 5 minutes at 200°C (about 1.3 μm of Si was removed) had an RMS roughness of about 30 nm. This roughness is similar to that observed using other fluorine-based etching techniques.[12,13]

To investigate the anisotropic nature of etching Si with our atomic fluorine beam, CaF_2 was used as an etch-resistant mask. For the CaF_2-masked Si(100) substrates, 1 μm-wide slots were opened in molecular-beam-epitaxially grown 20 nm-thick CaF_2 layers using electron-beam lithography following the procedure of Hirose *et al.*[14] In our case, a standard scanning electron microscope (SEM) with a 20 keV, 1 nA electron beam was used to write lines with a dose of 2.5 Ccm^{-2}. CaF_2 under direct electron-beam exposure dissociates leaving Ca, which oxidizes in air. The resist layer is then developed in water (CaO is 100 times more soluble in water than CaF_2) leaving 1 μm-wide openings to the underlying silicon. Figure 3(a) shows a cross-sectional SEM

view of a 1 μm-wide, 120 μm-deep trench in Si(100) fabricated by etching for 100 minutes with T_{SUB}=500°C. This trench is extremely anisotropic, with an aspect ratio of about 120:1 and a sidewall slope of about 1000:1 over nearly the entire depth. These aspect ratios and sidewall slopes were directly measured from SEM micrographs of samples cleaved along a plane intersecting the etched trench at a right angle and are comparable or higher than those currently achievable by reactive ion etching.[15,16] Another notable feature is that the 1.2 μm/min etch rate observed for the trench is within 20% of the open-area etch rate of 1.0 μm /min at 500°C (Fig. 2(b)). Since this is comparable to the run-to-run error of our experiments (see above), we conclude that our atomic beam does not exhibit appreciable aspect-ratio dependent etching (ARDE),[1] even for this high aspect-ratio geometry.

IV. DISCUSSION

In this section, we first discuss our open-area etch results, and second discuss our extremely anisotropic trenches obtained through etching through slot masks. In both cases we compare the result of this work to results obtained using other related techniques.

In this work, we find that the Si etch rate dependence on sample temperature and the etch selectivity to SiO_2 and Si_3N_4 are in qualitative agreement with those observed elsewhere.[11] Returning to the Arrhenius plot of Fig. 2, we note that our activation energy of 0.1 eV is in good agreement with Flamm *et al.*[11] However, we observe that there is a large disparity between the etch efficiencies for the different etching techniques. The right axis of the Arrhenius plot directly indicates the efficiency of Si removal by fluorine. (The arrows at 50% and 25% indicate an etch rate assuming unit efficiency for producing SiF_2 and SiF_4, respectively.) Based on our atomic fluorine flux, our etching efficiency is 3% for T_{SUB}=250°C, *i.e.*, one Si atom is removed for every

30 incident fluorine atoms. This is much higher than the 0.25% efficiency determined by Flamm *et al.*[11] (extrapolated to T_{SUB}=250°C) for etching with room-temperature atomic fluorine gas. Conversely, the results of Giapis *et al.*[5] demonstrate much higher efficiencies for an energetic fluorine beam generated by pulsed laser-induced dissociation of SF_6, even though this beam is incident upon a room-temperature substrate. We conclude that the etching rate is strongly dependent upon the incident kinetic energy of the atomic fluorine,[17] which averages 0.025 eV for Flamm *et al*. (0.25% efficiency), 1 eV for the present work (3% efficiency), and 5 eV for Giapis *et al*. (40% efficiency at room temperature). As discussed below, this energy dependent etch efficiency is important for the anisotropic etching results achieved in this work.

As noted in the Results Section associated with our highly anisotropic trench we observe two important features: 1) a lack of aspect ratio dependent etching (ARDE) and 2) a lack of sidewall etching. To understand this behavior we discuss and model the anisotropic etching process in terms of a highly collimated beam incident through a slot into the trench and the transport of the reacted and unreacted gas products out of the trench. Below we discuss and model this process to explain, first the lack of ARDE, and second the lack of sidewall etching.

The lack of observation of ARDE, even for the high aspect-ratio trench, may at first be surprising because ARDE is often observed for the usual medium-vacuum plasma techniques. However, in our beam technique, the incoming atoms in the beam will have little or no interaction with the trench walls. This is a consequence of the mask geometry and the fact that the beam is very well collimated. (This is in contrast to other gas-phase techniques where the interactions of the incident (uncollimated) reactive species with the trench walls are very important.) In the atomic beam case, it is the gas-gas phase interaction of the incident reactive F atoms with the effusive gas load from the trench bottom, which ultimately limits the depth of the trench for a given width. As

shown below, this lack of observation of ARDE in our experiments is showing that the mean-free-path length of the atomic F in the incident atomic beam in the trench (including the build up of pressure at the bottom of the trench) is larger than the depth of the trench itself. Adapting the procedure of Coburn and Winters,[18] the pressure at the trench bottom is determined in accordance with Knudsen transport by treating the trench bottom as a gas source and the trench itself as a conductance to the vacuum chamber at base vacuum. Note that implicit in considering Knudsen transport for the gas scattered from the trench bottom is the assumption that this gas will be randomly distributed in both energy and direction –in sharp contrast to the incident beam. This assumption is reasonable given that Hwang *et al.*[19] observed a largely cosine distributed scattered flux in their atomic F scattering experiments associated with both trapping desorption and indirect inelastic scattered fluorine.[20] In our case, because the trench bottom is not smooth, as discussed in the Results Section, even the direct scattering will tend to be random implying a cosine angular distribution. Using Q as the mass flow, or throughput, from the trench bottom that arises from the scattered incident beam, taking into account that by far the greatest contribution to this gas throughput is from the 95% He in the beam (the etch products themselves having negligible effect), we find that

$$Q = C\Delta p \approx kT\,\Phi_{He}\,ab, \qquad (1)$$

where F_{He} is the incident beam flux, a and b are the length and width of the trench, respectively, C is the trench conductance, Dp is the pressure difference between the trench bottom and outside the trench, and kT is included to convert from atoms/s to Torr-liter/s. The conductance for a slot with rectangular cross-section in the Knudsen flow regime is

$$C = K\frac{8}{3}\left(\frac{kT}{2\pi m}\right)^{1/2}\frac{ab^2}{L} \quad \text{for } a >> b, \qquad (2)$$

where L is the trench depth, T and m are the temperature and mass for the gas species, and K is an experimental geometry-dependent correction factor. Using (1) and (2) and rearranging we find

$$\Delta p = \frac{3}{8K}\left(2p\,m\,k\,T\right)^{1/2}\frac{\Phi_{He}L}{b}. \qquad (3)$$

Using K=2, F_{He}=1.3x10^{19} cm^{-2}s^{-1}, and m and T for He at the source temperature of 900^{o}C (1173 K) equation (3) gives a pressure difference of about 500 mTorr. This pressure difference, Dp, is essentially the pressure build-up at the bottom of the trench, p_t, because the pressure outside the trench (2x10^{-5} Torr) is negligible in comparison. Using the relationship between mean-free path length, l, and pressure from Ref. 21, and Eqn. (3), we find

$$l = \left(1+\frac{M_F}{M_{He}}\right)^{-1/2}\frac{kT}{p_t s_{He,F}} \propto \frac{b}{\Phi L}, \qquad (4)$$

where M_F and M_{He} are the atomic masses of F and He, respectively, and $s_{He\text{-}F}$ is the Helium-Fluorine cross section. Using M_F/M_{He}=19/4, T=1173 K, p_t=500 mTorr and $s_{He\text{-}F}$ = 0.2 nm^2, we find that the mean free path of the incident atomic fluorine in the beam is about 500 μm. (Note that in this calculation we used the gas temperature as that of the He in the source and neglected all but F-He scattering, however, taking T equal to the sample temperature, and including the other gas species has little effect on this outcome.) This mean-free-path length exceeds our trench depth by a factor of four, which explains the absence of gas-gas interactions leading to ARDE. Alternatively, by considering the probability of an incident F atom to undergo a collision as given by the mean-free-path length above, one finds that the probability of an incident F atom reaching 120 μm-depth *without* collision is about 90%. The ultimate depth attainable for a given trench width can be estimated by determining the depth at which this collision probability is about 50%. Under the conditions of the present experiment, this depth is about 250 μm for a 1 μm-wide opening of the trench. In addition, as indicated from Eqn. (4) the ultimate depth of a trench, L, would scale with

its width, *b*. In other words, the critical parameter for attaining a trench of a certain depth is its aspect ratio, *L/b*. For the beam flux used in this work, the ultimate aspect ratio is about 250:1, however, by reducing the incident flux, even higher aspect ratios should be possible. Finally, based on this analysis, such high aspect ratios can be obtained for much smaller trench openings, thus making this a viable technique to etch trenches on a nanoscale in silicon.

Regarding the observed lack of sidewall etching, for a collimated neutral beam, undercutting results from reactive species scattering within the trench and then striking and etching the sidewalls. As discussed above, for our pressure regime and geometry, gas phase interactions within the trench are not important. Only reactive species scattered from the trench bottom will contribute to sidewall etching. Given the relatively low efficiency of etching (7% at 500^{o}C), it is expected that there is substantial backscattered atomic fluorine. Again, as discussed above, as observed by Hwang *et al.*[19] and because the trench bottom is not smooth, it is a reasonable assumption that the reactive backscattered flux comes off with a cosine distribution. Therefore one can model the effect of this backscattered atomic fluorine by: treating *each* element of area on the trench bottom as a cosine distributed source of fluorine, $F_F dxdy$; integrating over the trench width, *x* from 0 to *b*, and length, *y* from -¥ to ¥ (we are interested in a very long trench) to determine the flux density of atomic fluorine at a point *z* on the sidewall as

$$P(z) = \frac{\Phi_F}{2}\left(1 - \frac{z}{\sqrt{z^2 + b^2}}\right), \qquad (5)$$

where *z=0* is the bottom of the trench; and finally (assuming a uniform etch rate, *m*, so that the depth of the trench, *z*, is given by *z=mt*, where *t* is the etch time) by integrating over the time corresponding to the time to etch from position *z* on the side wall to the final bottom of the trench, we find that the number density of fluorine atoms that hit the sidewall at a position z on the trench wall is

$$Q(z) = \frac{\Phi_F}{2m}\left(z + b - \sqrt{z^2 + b^2}\right). \quad (6)$$

The solid curve in Fig. 3(b) shows the trench profile calculated using this model with the assumption that the reactivity of backscattered fluorine is undiminished from that of fluorine incident upon the bottom of the trench. This profile shows a trench twice as wide as the mask opening with substantial curvature at the trench bottom. The dotted profile, calculated by assuming reduced reactivity of the scattered species by a factor of five, still shows widening, again with curvature at the bottom. The form of sidewall curvature given by this model is absent in our trenches. We do see etching of the sidewall at the top of the trench within about 3 μm of the mask, but this is clearly not of the form expected from scattered reactive species. In fact, the top feature appears to be the result of fluorine atoms that pass through pinholes in the CaF_2 mask near the trench opening and etch the Si. These pinholes are shown in the SEM micrograph Fig. 3(c).

This lack of sidewall etching observed in our trench is both qualitatively and quantitatively different from that observed by Giapis *et al.*, who use atomic F with much higher incident kinetic energies.[5,19] For F atoms incident at 5 eV, they see sidewall etching of about 14%, while this is reduced to about 3% for F atoms at 18 eV. Interestingly, we see much less sidewall etching even though our etch rate indicates a lower fluorine reaction efficiency. This implies that the large number of F atoms scattering from the bottom do not significantly etch the sidewalls in our case. Thus the observed lack of sidewall etching must result from reduced etching efficiency for F atoms scattered from the trench bottom, or to build-up of a passivation layer due to residual vacuum constituents, or to both. We believe that the former is much more likely, as we now discuss.

In order for atomic F to contribute to sidewall etching, the fluorine atoms incoming from the highly collimated beam must first strike the trench bottom, since the role of gas-gas collisions in the trench is negligible. Even partial energy accommodation with the surface will then deprive most of these F atoms of a considerable fraction of their incident 1 eV kinetic energy, so that

subsequent collisions with the sidewall will occur with much lower kinetic energy and at very large incident angles. Both these conditions would reduce sidewall etching efficiency. For example, based on the work of Flamm *et al.*,[11] extrapolated using Fig. 2(b), thermalized F atoms would etch Si at a rate of only about 0.1 μm/min (at 500°C), which is a factor of ten lower than our observed (downward) etching rate (thermalization at the substrate temperature of 500°C implies an average kinetic energy of 0.07 eV). Thus, from kinetic energy arguments alone, one would expect diffusively scattered fluorine to etch at a much slower rate than the atomic fluorine incident at 1 eV directly from the beam. Indeed, the magnitude of this variance in etch rates can by itself explain the sort of anisotropy we observe. The alternative possibility that sidewall etching is inhibited by build-up of a passivation layer from our non-UHV background is unlikely because, as discussed earlier, the ratio of background flux to the atomic fluorine beam flux is very low. Furthermore, this flux ratio on the sidewalls becomes even smaller as the trench gets deeper due to the slowness of Knudsen transport of background constituents down the trench. If the background vacuum was important, passivation would be more complete higher up the trench, and one would expect to see the trench widen as it goes deeper, which is not observed at all.

Trenches of the width and depth demonstrated here may be useful to micro electro-mechanical systems (MEMS) applications, as well as isolation trenches in integrated circuits. Of course this will require uniform etching over realistic wafer dimensions. This can be attained through a combination of increasing the beam size and rastering the wafer under the enlarged beam. The former can be accomplished by enlarging the skimmer, or by moving the sample further from the nozzle (Fig. 1), or both. Increasing the nozzle-sample distance increases the beam flux, which can be compensated by increasing the gas flow. It is the goal of future work to extend the use of this atomic-fluorine etching beam to an ultra-high vacuum sample environment. This will allow us

to investigate the origin of our lack of sidewall etching and to explore the feasibility of this technique to fabricate high aspect-ratio nanostructures.

V. SUMMARY and CONCLUSION

A neutral atomic fluorine beam was shown to produce etch rates in silicon as high as 1 μm/min. Using a CaF_2 resist layer we fabricated 120 μm-deep by 1 μm-wide trenches (aspect ratio 120:1) in silicon with no appreciable sidewall taper (slopes of about 1000:1) or ARDE effects. Achieving such anisotropic etching suggests that scattered species do not contribute significantly to sidewall etching, *i.e.* the vast majority of etching is caused by the highly directional incident atomic-fluorine beam. Although sidewall passivation caused by background vacuum constituents could be inhibiting sidewall etching, we show that this is unlikely due to the much larger flux directed at the substrate by the collimated atomic fluorine beam. We calculate that the ultimate depth attainable for a 1 μm-wide trench is about 250 μm, and we show that the critical parameter for the ultimate depth of a trench is its aspect ratio. This suggests that our etching technique can be used to fabricate trenches on a nanoscale, while maintaining aspect ratios of 100 or greater.

ACKNOWLEDGMENTS

We thank X.M. Fang and P.J. McCann for the thin CaF_2 films on Si(100) and R.T. Collins for valuable conversations. This research was supported under NSF grant number CHE-9405005 (to MK); acknowledgement is also made to the donors of the Petroleum Research Fund, administered by the American Chemical Society, for partial support of this research (to MK).

Figures

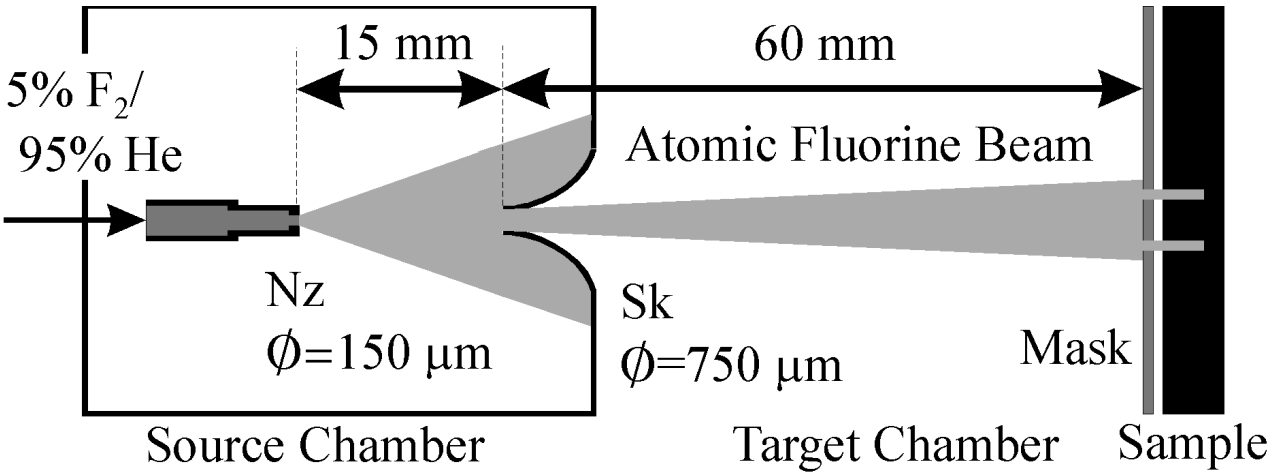

FIG. 1. Schematic of atomic fluorine beam etching apparatus. A high-pressure (2000-3000 Torr) gas mixture of 5% molecular fluorine in helium is introduced into a MgF_2 tube heated to 900°C. At this temperature approximately 70% of the molecular fluorine dissociates into atomic fluorine. The gas mixture then expands through the 150 μm-diameter nozzle (Nz). The 750 μm-diameter skimmer (Sk) collimates the gas into a beam, which impinges on the masked sample in the target chamber. The energy of the atomic fluorine in the beam is about 1.0±0.1eV, and the flux at the target is about $1x10^{18}$ $cm^{-2}s^{-1}$. Based on the diameter of the source nozzle and target position, the angular dispersion is 0.1^o.

F

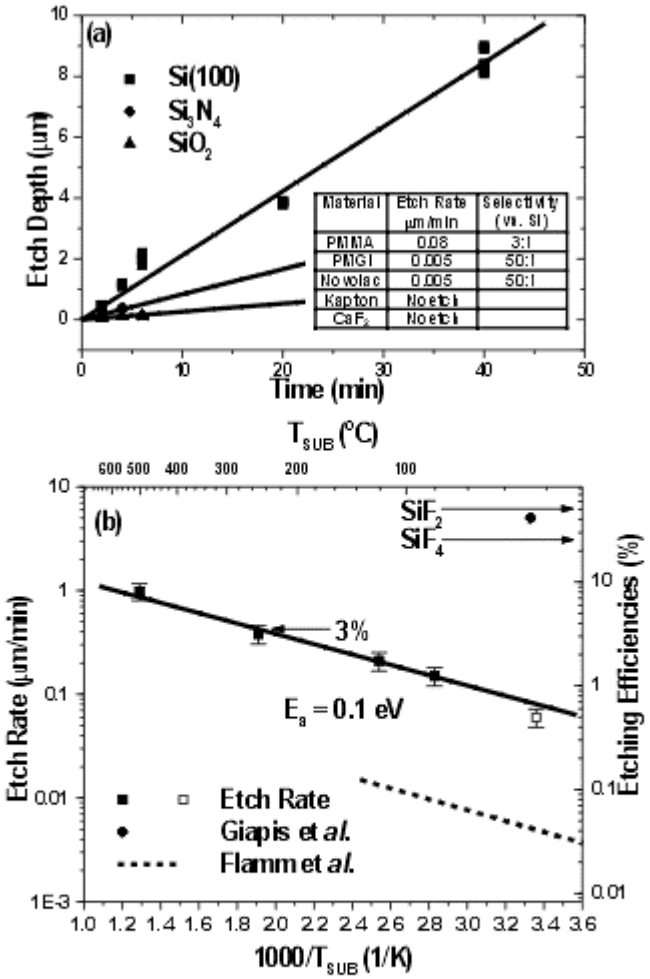

IG. 2. (a) Etch depth vs. time for silicon, Si_3N_4 and SiO_2 at T_{SUB}=120°C. Measured etch rates of resists at 200°C given in table (inset). (b) An Arrhenius plot showing silicon etch rate versus $1000/T_{SUB}$. Our results are shown with a solid line through solid squares. Room temperature etch rate is shown as an open square. The arrows indicate etch efficiencies for silicon assuming two (four) fluorine atoms for every silicon atom removed, *i.e.* SiF_2 (SiF_4). Results shown for Flamm *et al.*[11] (dashed line) and Giapis *et al.*[5] (solid circle) are normalized to our flux in order to compare etching efficiencies.

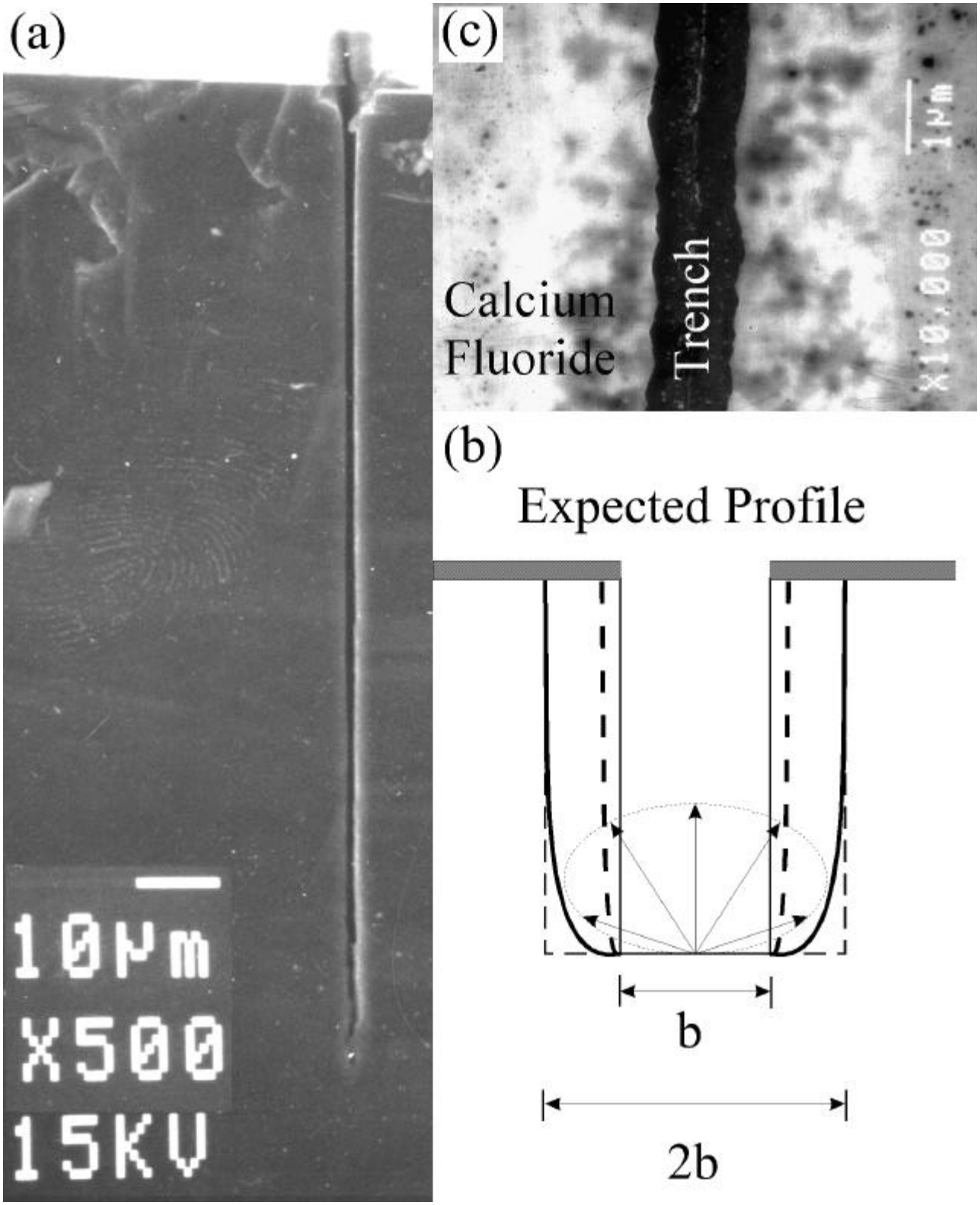

FIG. 3. (a) Cross-sectional SEM view of a 1 μm wide, 120 μm-deep, CaF_2-masked trench in Si(100). (b) Shows a plot of the expected profile assuming a cosine distribution for reactive species scattered at the bottom of the trench with the solid (dotted) line for full (20%) reactivity. (c) Shows a top view of the trench and the CaF_2 mask, as labeled. Note the pinholes in the CaF_2 mask.

References

1. R. A. Gottscho, C. W. Jurgensen, and D. J. Vitkavage, J. Vac. Sci. Technol. B **10**, 2133 (1992).

2. T. Nozawa, T. Kinoshita, T. Nishizuka, A. Narai, T. Inoue, and A. Nakaue, Jpn. J. Appl. Phys. **34**, 2107 (1995).

3. G. Dharmasena, K. Copeland, J. H. Young, R. A. Lasell, T. R. Phillips, G. A. Parker, and M. Keil, J. Phys. Chem. A **101**, 6429 (1997); M. Keil, J. H. Young, and K. Copeland, "Method and Apparatus for Etching Surfaces with Atomic Fluorine" *U. S. Patent #5,597,495*.

4. M. Faubel, B. Martinez-Haya, L.Y. Rusin, U. Tuppe, and J. P. Toennies, J. Phys. D: Appl. Phys. **29**, 1885 (1996).

5. K. P. Giapis, T. A. Moore, and T. K. Minton, J. Vac. Sci. Technol. A **13**, 959 (1995).

6. R. J. Levis, C. J. Waltman, L. M. Cousins, R. G. Copeland, and S. R. Leone, J. Vac. Sci. Tech. A, 3118 (1990).

7. Szabo, P. D. Farrall, and T. Engel, J. Appl. Phys., 3623 (1994).

8. M. Faubel, B. Martinez-Haya, L. Y. Rusin, U. Tappe, and J.P. Toennies, J. Phys. Chem. **A 101**, 6415 (1997).

9. J.F. O'Hanlon, in *A Users Guide to Vacuum Technology*, 2nd ed., John Wiley & Sons, New York, 1989),p. 466.

10. The Si samples were run longer than the Si_3N_4 and SiO_2 because the latter were only available as thin films.

11. D. L. Flamm, V. M. Donnelly, and J. A. Mucha, J. Appl. Phys. **52**(5), 3633 (1981).

12. R. Petri, P. Brault, O. Vatel, D. Henry, E. Andre, P Dumas, and F. Salvan, J. Appl. Phys.**75**(11), 7498 (1994).

13. M. J. M. Vugts, M. F. A. Eurlings, L. J. F. Hermans, and H. C. W. Beijerinck, J. Vac. Sci. Technol. A **14**(5), 2780 (1996).

14. Y. Hirose, S. Horng, A. Kahn, C. Wrenn, and R. Pfeffer, J. Vac. Sci. Technol. A **10**(4), 960 (1992).

15. A. G. Nassiopoulos, S. Grigoropoulos, E. Gogolides, and D. Papadimitriou, Appl. Phys. Lett. **66**(9), 1114 (1995).

16. J. K. Bhardwaj, H. Ashraf, Proceedings of the SPIE **2639**, 224 (1995).

17. Due to the difficulty in measuring beam flux, etching efficiencies for beam techniques have much larger errors (*e.g.*, a factor of 2 for our results) than the data of Flamm *et a.l*. However, this factor of 2 error is much smaller than the ~10x enhancement observed over the data of Flamm *et al*..

18. J. W. Coburn and H. F. Winters, Appl. Phys. Lett. **55**, 2730 (1989).

19. G. S. Hwang, C. M. Anderson, M. J. Gordon, T. A. Moore, T. K. Minton, and K. P. Giapis, Phys. Rev. Lett. **77**, 3049 (1996).

20. From Hwang *et al.* deconvolution of their scattering data suggests three distinct scattering processes: 1) direct inelastic scattering with a Gaussian angular distribution about the specular direction, and 2) indirect inelastic scattering and 3) trapping desorption, both with approximately cosine angular distributions

21. G. L. Weissler and R. W. Carlson, in *Vacuum Physics and Technology*, Volume 14, Academic Press, New York, 1979.